

# Two-Timescale Channel Estimation for RIS-Aided Near-Field Communications

Jeongjae Lee, *Student Member, IEEE* and Songnam Hong, *Member, IEEE*

**Abstract**—In this paper, we investigate the channel estimation problem in reconfigurable intelligent surface (RIS)-aided near-field communication systems, where the extremely large number of RIS elements imposes considerable pilot overhead and computational complexity. To address this, we employ a two-timescale channel estimation strategy that exploits the asymmetric coherence times of the RIS-base station (BS) channel and the User-RIS channel. We derive a time-scaling property indicating that for any two effective channels within the longer coherence time, one effective channel can be represented as the product of a vector, referred to as the small-timescale effective channel, and the other effective channel. By utilizing the estimated effective channel along with processed observations from our piecewise beam training, we present an efficient method for estimating subsequent small-timescale effective channels. We theoretically establish the efficacy of the proposed RIS design and demonstrate, through simulations, the superiority of our channel estimation method in terms of pilot overhead and computational complexity compared to existing methods across various realistic channel models.

**Index Terms**—Reconfigurable intelligent surface, near-field communications, channel estimations.

## I. INTRODUCTION

With the growth of various emerging applications such as autonomous vehicles, virtual reality, and holograms, future wireless communication systems aim to support ultrahigh data rates [1]–[3]. To this end, it is imperative to develop an efficient technique to mitigate severe pathloss in high-frequency communications, such as millimeter wave (mmWave) and terahertz (THz) [4], [5]. The extremely large-scale antenna array (ELAA) has been proposed to substantially enhance beamforming gain in massive multiple-input multiple-output (MIMO) systems, thereby effectively mitigating loss [6]. In MIMO systems with ELAA, referred to as XL-MIMO, hundreds to thousands number of antennas form a uniform antenna array, enabling to generate specific beam patterns. Additionally, a reconfigurable intelligence surface (RIS), positioned between a base station (BS) and users, can physically enhance blocked or weakened channels by favorably manipulating incident waves, thereby improving overall communication performance [7]–[9]. Owing to its lower implementation costs and power consumptions, this technology is considered for

overcoming the physical limitations of high-frequency communications by establishing new and strengthened channels.

By leveraging the advantages of both techniques, the integration of ELAA and RIS has been recently explored in the current literature [10], [11]. In contrast to conventional RIS-aided communication systems, such as RIS-aided MIMO systems [12], the spherical near-field effect must be considered due to the electromagnetic characteristic of ELAA [13]. This integrated system is designated as the RIS-aided *near-field* communication system and exhibits characteristics akin to a double-edged sword. Enhanced by a high-rank line-of-sight (LoS) channel and precise beamfocusing capability, there exists a novel opportunity in RIS-aided near-field communication systems that improves the degree of freedom (DoF) [10]. Nevertheless, estimating the channels or optimizing beam focusing becomes extremely challenging due to the significantly increased number of parameters associated with higher rank [14], as well as the notable emergence of substantial beam splitting or beam squint in wideband systems [15], [16]. We in this paper contribute to the channel estimation problem in RIS-aided near-field MIMO systems.

### A. Related Works

Over the past five years, the channel estimation problem for the RIS-aided MIMO systems has been widely investigated [17]–[22]. The objective is to acquire the channel between the RIS and the base station (BS), referred to as the RIS-BS channel, as well as the channels between the users and the RIS, termed the User-RIS channels. However, estimating these channels separately is impractical due to the lack of a signal processing unit at the RIS. Considering both practicality and usefulness, existing works have concentrated on estimating the effective (or cascaded) channels while maintaining an affordable pilot overhead. Herein, each effective channel is defined as the product of the RIS-BS channel matrix, the diagonal phase shift matrix—which mathematically represents the physical effects of the RIS—and the User-RIS channel matrix. To develop an efficient channel estimation method, one representative approach is to leverage the sparsity of mmWave or THz channels. This sparsity arises from the presence of a dominant line-of-sight (LoS) path coupled with a limited number of non-line-of-sight (NLoS) signal paths in the RIS-BS channel. The most popular channel estimation method utilizing the sparsity is based on compressed sensing (CS) [17], [23]. In [17], the effective channel was well-approximated as a row-wise and column-wise sparse matrix using the virtual angular domain representation. Subsequently, CS algorithms,

J. Lee and S. Hong are with the Department of Electronic Engineering, Hanyang University, Seoul, Korea (e-mail: {lyjcje7466, shong}@hanyang.ac.kr).

This work was supported in part by the Technology Innovation Program (1415178807, Development of Industrial Intelligent Technology for Manufacturing, Process, and Logistics) funded By the Ministry of Trade, Industry & Energy (MOTIE, Korea) and in part by the Institute of Information & Communications Technology Planning & Evaluation (IITP) under the artificial intelligence semiconductor support program to nurture the best talents (IITP-(2024)-RS-2023-00253914) grant funded by the Korea government(MSIT).

such as orthogonal matching pursuit (OMP), were directly applied. Furthermore, the super-resolution (SR) method utilizing atomic norm minimization (ANM) was introduced, enhancing the performance of the CS-based method by mitigating the grid-mismatch problem [18]. These sparsity-based methods demonstrate significant performance improvements for the *far-field* effective channels, where array response vectors are linear with respect to channel parameters such as the angle-of-arrival (AoA) and angle-of-departure (AoD) in the planar wave approximation.

Despite the channel sparsity, employing the compressive sensing (CS) framework in RIS-aided near-field MIMO systems presents significant challenges. This difficulty arises from the non-linearity of the near-field array response vector, which is a consequence of its spherical wavefronts. In [19], [20], this challenging problem was examined under an ideal scenario: the LoS far-field RIS-BS channel is known a priori, while the near-field User-RIS channels are solely estimated. In this scenario, a CS-based channel estimation method was proposed for the RIS-aided near-field MU-MIMO systems with hybrid beamforming architecture, leveraging the polar-domain sparsity introduced in [14], [24]. Notably, the dictionary matrix differs significantly from those used in CS-based far-field counterparts [17], [18], as it must be carefully designed according to the structures of the array response vectors. For practicality, it is essential to design a more effective channel estimation method that does not require any prior knowledge and can operate in both near-field and far-field RIS-BS channels. Recently in [21], an efficient channel estimation method, referred to as CLRA, was proposed for RIS-aided near-field MIMO systems (also known as XL-RIS assisted XL-MIMO systems). This method was developed by leveraging the low-rankness of the RIS-BS channel. Remarkably, the CLRA can be seamlessly applied to both far-field and near-field channels without any modification, whereas CS-based methods necessitate a suitable design of the dictionary matrix tailored to the categories of wireless channels. Furthermore, it has been demonstrated that the CLRA achieves higher estimation accuracy in far-field, near-field, and mixed far-field/near-field channels compared to the corresponding CS-based methods, all while maintaining lower training overhead.

### B. Our Contributions

In this paper, we investigate a channel estimation problem for RIS-aided MU-MIMO systems utilizing a hybrid beamforming structure. For the sake of practicality, we consider various channel models, including i) a typical low-rank or sparse far-field channel; ii) a mixed LoS/NLoS near-field channel [22], [24]; iii) a spatial non-stationary near-field channel [25]. As summarized in Section I-A, the existing methods can be employed for these types of channels. However, they still require substantial pilot overheads, rendering them impractical, especially when the number of RIS elements becomes considerably large [10], [19], [20], [22]. To further mitigate pilot overhead in a near-field channel, a two-timescale channel estimation method was proposed in [26], by leveraging the asymmetry between the coherence times of the RIS-BS and

the User-RIS channels. However, this method is applicable only when the BS operates at full-duplex mode, which limits its practicality across various RIS-aided MIMO systems. Furthermore, no theoretical analysis for the design of the RIS reflection vector was provided.

Motivated by the aforementioned considerations, we investigate a channel estimation method suitable for the two-time channel estimation (denoted as 2TCE) framework, particularly when the BS operates at half-duplex mode and employs a hybrid beamforming architecture. The 2TCE framework consists of two phases: i) large-timescale channel estimation; ii) small-timescale channel estimation. Within the coherence time of the RIS-BS channel, the former estimation is performed only once, while the latter estimation is conducted several times. In this paper, we propose a novel small-scale channel estimation method that achieves higher accuracy and reduced training overhead. Our major contributions are summarized as follows:

- We derive a time-scaling property, indicating that for any two effective channels within the coherence time, one effective channel can be represented by the product of a vector, called the small-timescale effective channel, and the other effective channel. Consequently, once the first effective channel is estimated, the subsequent effective channels can be recovered by estimating small-timescale effective channels with lower dimensions.
- For large-timescale channel estimation, we employ the state-of-the-art (SOTA) channel estimation method proposed in [22], referred to as PW-CLRA, which exhibits attractive performance for both far-field and near-field channels. It is important to note that any channel estimation method, including CS-based methods, can be also adopted as the large-timescale channel estimation method.
- As our primary contribution, we present an efficient method for estimating subsequent small-timescale effective channels, along with the design of RIS reflection vectors that are suitable for the proposed method. Furthermore, we provide a preliminary theoretical analysis of our RIS design, offering guidelines for selecting a hyperparameter. The proposed 2TCE method, based on the time-scaling property, is designated as 2TCE-TSP.
- Through simulations, we verify the superiority of the proposed 2TCE-TSP method across various channels. Notably, this method achieves a 50% and 75% reduction from the pilot overhead of SOTA method [22]. When compared to the existing 2TCE method proposed in [26], the proposed method attains significant performance gains across all pilot overhead regimes while maintaining substantially lower computational complexity, achieving a reduction of approximately 70% when using 256 RIS elements.

The remaining part of this paper is organized as follows. In Section II, we define the signal model for RIS-aided MU-MIMO systems, incorporating a hybrid beamforming structure, and present our channel estimation framework, dubbed 2TCE. In Section III, we review PW-CLRA as the large-timescale channel estimation method within our 2TCE frame-

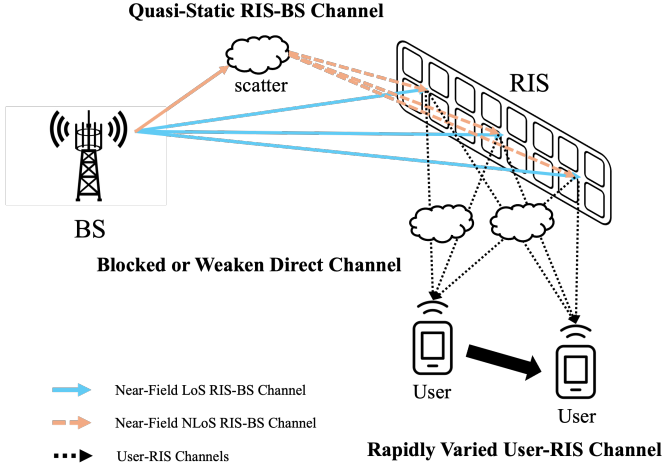


Fig. 1. The description of the RIS-aided MU-MIMO systems.

work. Section IV provides a detailed outline of the proposed small-timescale channel estimation method. In Section V, we analyze the proposed channel estimation method with regard to its computational complexity and pilot overhead. Section VI provides simulation results and Section VII concludes the paper.

*Notations.* Let  $[N_1 : N_2] \triangleq \{N_1, N_1 + 1, \dots, N_2\}$  for any integer  $N_1, N_2$  with  $N_2 > N_1$ . For  $N_1 = 1$ , this notation simplifies to  $[N_2]$ . We use  $\mathbf{x}$  and  $\mathbf{A}$  to denote a column vector and matrix, respectively. Also,  $\circ$  denotes the Hadamard product. Given a  $M \times N$  matrix  $\mathbf{A}$ , let  $\mathbf{A}(i, :)$  and  $\mathbf{A}(:, j)$  denote the  $i$ -th row and  $j$ -th column of  $\mathbf{A}$ , respectively. Given  $m < M$  and  $n < N$ , let  $\mathbf{A}([m], :)$  and  $\mathbf{A}(:, [n])$  denote the submatrices by taking the first  $m$  rows and  $n$  columns of  $\mathbf{A}$ , respectively. Also,  $\text{Rank}(\mathbf{A})$ ,  $\mathbf{A}^H$ ,  $\|\mathbf{A}\|_2$ ,  $\|\mathbf{A}\|_F$  denote the rank, the Hermitian transpose, the  $\ell_2$ -norm, and the Frobenius norm of  $\mathbf{A}$ , respectively. Given a vector  $\mathbf{v}$ ,  $\mathbf{v}^*$  denotes the complex conjugate vector of  $\mathbf{v}$  and  $\text{diag}(\mathbf{v})$  denotes a diagonal matrix whose  $\ell$ -th diagonal element corresponds to the  $\ell$ -th element of  $\mathbf{v}$ . Without loss of generality, it is assumed that in the diagonal matrix resulting from the eigenvalue decomposition, the diagonal elements, which correspond to the eigenvalues, are arranged in descending order based on their absolute values.

## II. PRELIMINARIES

As shown in Fig. 1, we consider a mmWave MIMO system operating in time division duplex (TDD) mode, in which a base station (BS) serves  $K$  mobile users. The BS is equipped with  $N$  antennas, while the users are all equipped with a single antenna. Due to a severe path loss in mmWave or THz communications, the direct channel between the BS and the users is typically blocked or weakened. To overcome this limitation, we assume that a reconfigurable intelligent surface (RIS), positioned between the BS and the users, assists the communications between them by favorably manipulating the incident waves. The RIS is equipped with  $M$  antennas connected to an  $M$ -port single connected reconfigurable networks (a.k.a. the conventional diagonal RIS).

In this paper, we aim to develop a channel estimation method for the deployment of the aforementioned RIS-assisted communications. To this end, we will present a signal model along with the proposed strategy for developing a channel estimation method in the subsequent subsections. In TDD systems, the downlink channels are derived from the uplink channel estimation due to the channel reciprocity. Therefore, our channel estimation method will be articulated based on the uplink channel estimation protocol. To enhance clarity, we shall elucidate the proposed channel estimation method in the context of a single-user setting. However, this method can be readily extended to a multi-user scenario through the use of orthogonal pilots.

### A. Signal Model

To mitigate complexity and power consumption, the BS is assumed to be equipped with a hybrid beamforming architecture, where all receive antennas share the limited number of radio frequency (RF) chains, denoted as  $N_{\text{RF}} \ll N$ . Then, the uplink signal from the user to the BS via the RIS can be expressed in the baseband representation as follows:

$$\begin{aligned} \mathbf{y} &= \mathbf{W}^{\text{RF}} (\mathbf{H}^{\text{RB}} \text{diag}(\mathbf{v}) \mathbf{h}^{\text{UR}}_s + \mathbf{n}) \\ &\stackrel{(a)}{=} \mathbf{W}^{\text{RF}} (\mathbf{H}^{\text{eff}} \mathbf{v}_s + \mathbf{n}) \in \mathbb{C}^{N_{\text{RF}} \times 1}, \end{aligned} \quad (1)$$

where  $s \in \mathbb{C}$  is the transmit signal at the user, with the transmit power constraint as  $|s|^2 = P$ ,  $\mathbf{h}^{\text{UR}} \in \mathbb{C}^{M \times 1}$  denotes the channel from the user to the RIS (in short, User-RIS channel),  $\mathbf{v} \in \mathbb{C}^{M \times 1}$  is the RIS reflection vector,  $\mathbf{H}^{\text{RB}} \in \mathbb{C}^{N \times M}$  denotes the channel from the RIS to the BS (in short, RIS-BS channel), and  $\mathbf{W}^{\text{RF}} \in \mathbb{C}^{N_{\text{RF}} \times N}$  is the analog combiner at the BS. Also, the equality in (a) comes from the fact that the total cascaded channel can be transformed as:

$$\mathbf{H}^{\text{RB}} \text{diag}(\mathbf{v}) \mathbf{h}^{\text{UR}} = \mathbf{H}^{\text{RB}} \text{diag}(\mathbf{h}^{\text{UR}}) \mathbf{v} = \mathbf{H}^{\text{eff}} \mathbf{v}, \quad (2)$$

where  $\mathbf{H}^{\text{eff}} \triangleq \mathbf{H}^{\text{RB}} \text{diag}(\mathbf{h}^{\text{UR}}) \in \mathbb{C}^{N \times M}$  is referred as the *effective channel* in this paper. Noticeably, both the analog combiner  $\mathbf{W}^{\text{RF}}$  and the RIS reflection vector  $\mathbf{v}$  adhere to the constant modulus constraint, where each element has the same magnitude as follows:

$$|\mathbf{W}^{\text{RF}}(i, j)| = 1/\sqrt{N} \text{ and } |\mathbf{v}(m)| = 1, \quad (3)$$

for all  $i \in [N^{\text{RF}}]$ ,  $j \in [N]$ , and  $m \in [M]$ .

### B. Channel Estimation Strategy

Noticeably, the BS and the RIS are respectively positioned in fixed locations, while the mobile user rapidly moves, which results in an asymmetry between the channel coherence time of the RIS-BS channel and the User-RIS channel. The RIS-BS channel is characterized as quasi-static, thereby necessitating estimation over a larger timescale. On the contrary, the User-RIS channel exhibits time variation attributable to user mobility, thereby requiring estimation on a smaller timescale. Throughout the paper, the coherence times of the RIS-BS and User-RIS channels are denoted as  $T^{\text{RB}}$  and  $T^{\text{UR}}$ , respectively. Additionally, the ratio  $T = T^{\text{RB}}/T^{\text{UR}}$  is assumed to be a positive integer. Within the longer coherence time  $T^{\text{RB}}$ , there

exists a sequence of  $T$  User-RIS channels, denoted as  $\mathbf{h}_t^{\text{UR}}$  for  $t \in [0 : T - 1]$ . Consequently, from (2), the sequence of effective channels is represented as  $\mathbf{H}_t^{\text{eff}} = \mathbf{H}^{\text{RB}} \text{diag}(\mathbf{h}_t^{\text{UR}})$  for  $t \in [0 : T - 1]$ .

From this, we can derive the *time-scaling property*, which indicates that each  $\mathbf{H}_t^{\text{eff}}$  can be expressed as the product of the initial effective channel  $\mathbf{H}_0^{\text{eff}}$  and a time-specific  $M \times 1$  vector:

$$\begin{aligned} \mathbf{H}_t^{\text{eff}} &= \mathbf{H}^{\text{RB}} \text{diag}(\mathbf{h}_0^{\text{UR}}) \text{diag}(\mathbf{d}_t) \\ &= \mathbf{H}_0^{\text{eff}} \text{diag}(\mathbf{d}_t), \end{aligned} \quad (4)$$

where the small-timescale effective channel is defined as:

$$\mathbf{d}_t \triangleq \text{diag}(\mathbf{h}_0^{\text{UR}})^{-1} \mathbf{h}_t^{\text{UR}} \in \mathbb{C}^{M \times 1}. \quad (5)$$

By harnessing this property, we introduce a two-timescale channel estimation framework, referred to as 2TCE. This framework consists of two phases:

- *Large-timescale channel estimation:* Utilizing the SOTA channel estimation method [22], we estimate the large-timescale effective channel matrix during the initial time block, which is denoted as  $\hat{\mathbf{H}}_0^{\text{eff}}$ .
- *Small-timescale channel estimation:* As the main contribution of this paper, we estimate the subsequent small-timescale effective channels by leveraging the initially estimated large-timescale effective channel. The estimated channels are denoted as  $\hat{\mathbf{d}}_t$ , where  $t \in [T - 1]$ .

We note that the pilot overhead necessary for estimating the small-timescale effective channels, which comprises  $M$  channel parameters, is considerably smaller than that required for the large-timescale effective channel, which includes  $NM$  channel parameters. In addition, the 2TCE strategy can be directly utilized in the two-timescale beamforming optimization and RIS design, which has been extensively studied in the current literature [27], [28].

As the most relevant work, a 2TCE method (dubbed 2TCE-FD) was proposed in [26], wherein  $\mathbf{H}^{\text{RB}}$  is estimated using dual-link pilot transmission as large-timescale channel estimation, under the assumption that the BS works at full-duplex mode [29]. Specifically, the BS transmits pilots to the RIS via the downlink channel with a single transmit antenna, and then the RIS reflects these pilot signals back to the BS through the uplink channel. Simultaneously, the BS also receives pilots using its remaining antennas. The BS can estimate  $\mathbf{H}^{\text{RB}}$  from the reflected signals. Also, the subsequent effective channels are recovered by estimating only the  $M \times 1$  vector  $\mathbf{h}_t^{\text{UR}}$  for  $t \in [T - 1]$  as small-timescale channel estimation, given that  $\mathbf{H}^{\text{RB}}$  remains unchanged. Assuming that BS is equipped with a fully-digital beamforming structure (i.e.,  $N_{\text{RF}} = N$ ), it follows that the minimum pilot overhead amounts to  $2M$  for large-timescale channel estimation. Furthermore, it is evident that when employing a hybrid beamforming architecture, the minimum pilot overhead increases by a factor of  $N/N_{\text{RF}}$ . Throughout the paper, the *minimum pilot overhead* refers to the required number of pilot signal transmissions to perform an associated channel estimation method. To suitably utilize the full-duplex system at the BS, the self-interference issue must be addressed using existing interference suppression methods

[29]–[31], which incur additional computational costs. Therefore, in this paper, we focus on a more practical scenario aimed at estimating effective channels in the half-duplex mode, consistent with most related works. To implement this concept in a standard BS operating at half-duplex mode, we employ the time-scaling property described in (4), which facilitates the recovery of effective channels in subsequent time blocks by estimating only the  $M \times 1$  vector  $\mathbf{d}_t$  for  $t \in [T - 1]$ .

### III. LARGE-TIMESCALE CHANNEL ESTIMATION

In this section, we elucidate the piecewise low-rank approximation, which was initially introduced in [22] as the primary component to estimate a large-timescale effective channel. Referred as the RIS-aided near-field communications, both the RIS-BS channel and the User-RIS channel typically exhibit near-field channels due to the extremely enlarged antenna aperture of the RIS for achieving significant high data rates [10], [11], [13]. This near-field characteristic results in a loss of channel sparsity or low-rankness, which is a crucial property for substantially reducing pilot overhead in the existing methods [17]–[21]. In [22], to relax the high-rank nature of the RIS-BS channel  $\mathbf{H}^{\text{RB}}$ , the effective channel in the initial time block is divided into  $Q$  distinct piecewise effective channels  $\{\mathbf{H}_{[q,0]}^{\text{pw}} : q \in [Q]\}$  as follows:

$$\mathbf{H}_0^{\text{eff}} = \begin{bmatrix} \mathbf{H}_{[1,0]}^{\text{pw}} & \cdots & \mathbf{H}_{[Q,0]}^{\text{pw}} \end{bmatrix}, \quad (6)$$

where

$$\mathbf{H}_{[q,0]}^{\text{pw}} \triangleq \mathbf{H}_q^{\text{RB}} \text{diag}(\mathbf{h}_{[q,0]}^{\text{UR}}) \in \mathbb{C}^{N \times M_{\text{sub}}}, \quad (7)$$

for  $q \in [Q]$  and  $M_{\text{sub}}Q = M$ . Herein, we have:

$$\mathbf{H}_q^{\text{RB}} = \mathbf{H}^{\text{RB}}(:, \mathcal{M}_q) \text{ and } \mathbf{h}_{[q,0]}^{\text{UR}} = \mathbf{h}_0^{\text{UR}}(\mathcal{M}_q), \quad (8)$$

where  $\mathcal{M}_q = \{1 + (q - 1)M_{\text{sub}} : qM_{\text{sub}}\}$ . Then, each piecewise effective channel can be decomposed as:

$$\mathbf{H}_{[q,0]}^{\text{pw}} = \mathbf{S}_q \mathbf{T}_{[q,0]}, \quad (9)$$

where  $\mathbf{S}_q$  is an  $N \times r_q$  matrix whose  $r_q$  columns span the column space of  $\mathbf{H}_q^{\text{RB}}$  and  $\mathbf{T}_{[q,0]} \in \mathbb{C}^{r_q \times M_{\text{sub}}}$  is the coefficient matrix associated to  $\mathbf{S}_q$ . By leveraging the SOTA channel estimation algorithm (dubbed PW-CLRA) proposed in [22], the effective channel in the initial time block can be efficiently estimated, which is denoted as

$$\hat{\mathbf{H}}_0^{\text{eff}} = \begin{bmatrix} \hat{\mathbf{H}}_{[1,0]}^{\text{pw}} & \cdots & \hat{\mathbf{H}}_{[Q,0]}^{\text{pw}} \end{bmatrix}. \quad (10)$$

Given that  $\mathbf{S}_q$  is accurately approximated as a low-rank matrix, the SOTA method estimates the piecewise effective channels while ensuring a short pilot overhead, in the following ways:

$$\begin{aligned} \hat{\mathbf{H}}_{[q,0]}^{\text{pw}} &= \hat{\mathbf{S}}_q \hat{\mathbf{T}}_{[q,0]} \\ &= \mathbf{H}_q^{\text{pw}} + \mathbf{\Delta}_{[q,0]}, \end{aligned} \quad (11)$$

where  $\hat{\mathbf{S}}_q \in \mathbb{C}^{N \times \hat{r}_q}$  and  $\hat{\mathbf{T}}_{[q,0]} \in \mathbb{C}^{\hat{r}_q \times M_{\text{sub}}}$  are estimated by means of piecewise low-rank approximation with the estimated rank  $\hat{r}_q$  [22], and  $\mathbf{\Delta}_{[q,0]} \in \mathbb{C}^{N \times M_{\text{sub}}}$  denotes the channel estimation error. In future wireless networks, a dense mobile user scenario (i.e.,  $K \gg 1$ ) is typically assumed. Consequently, the PW-CLRA algorithm is capable of mitigating the

channel estimation error, leveraging the multi-user gains for the estimation of  $\mathbf{S}_q$ . For the sake of brevity in describing the proposed channel estimation method in Section IV, nonetheless, we will disregard the impact of channel estimation errors (i.e.,  $\hat{r}_q = r_q$  and  $\Delta_{[q,0]} = 0$ ). However, these effects will be thoroughly investigated in our simulations. As derived in [22], the minimum pilot overhead of the PW-CLRA is expressed as  $Q(N/N_{\text{RF}}) + M$ , where the first term  $Q(N/N_{\text{RF}})$  and the second term  $M$  are demanded for the estimations of  $\{\mathbf{S}_q : q \in [Q]\}$  and  $\{\mathbf{T}_{[q,0]} : q \in [Q]\}$ , respectively. By selecting the hyperparameter  $Q$ , one can effectively manage the tradeoff between estimation accuracy and pilot overhead.

#### IV. SMALL-TIMESCALE CHANNEL ESTIMATION

Based on the estimated matrix  $\hat{\mathbf{S}}_q$  in (11), we can model the subsequent effective channels as follows:

$$\mathbf{H}_{[q,t]}^{\text{PW}} = \hat{\mathbf{S}}_q \mathbf{T}_{[q,t]}, \quad (12)$$

for  $t \in [T-1]$  and  $q \in [Q]$ . During the time block  $t \geq 1$ , we can recover the effective channel by only estimating the coefficient matrix  $\mathbf{T}_{[q,t]}$  for  $q \in [Q]$ . This can be efficiently derived using the least square (LS) or joint optimization (JO) solution, outlined in [22]. This two-phase channel estimation method based on PW-CLRA is referred to as 2TCE-PWCLRA. From this, the minimum pilot overhead of 2TCE-PWCLRA per each time block can be reduced to  $M$ . Without leveraging the additional capabilities offered by full-duplex mode, the 2TCE-PWCLRA requires a lower pilot overhead compared to the 2TCE-FD proposed in [26]. Nevertheless, the reduced pilot overhead  $M$  of 2TCE-PWCLRA would become unaffordable as the number of RIS elements increases considerably.

Motivated by the above, we propose an efficient small-timescale channel estimation method that offers an attractive pilot overhead below  $M$ , which is the main contribution of this paper. By leveraging the time-scaling property in (4), we derive the time-scaling property in a piecewise manner as follows:

$$\begin{aligned} \mathbf{H}_{[q,t]}^{\text{PW}} &= \mathbf{H}_q^{\text{RB}} \text{diag}(\mathbf{h}_{[q,t]}^{\text{UR}}) \\ &= \mathbf{H}_{[q,0]}^{\text{PW}} \text{diag}(\mathbf{d}_{[q,t]}), \end{aligned} \quad (13)$$

where the piecewise small-timescale effective channel is defined as:

$$\mathbf{d}_{[q,t]} \triangleq \text{diag}(\mathbf{h}_{[q,0]}^{\text{UR}})^{-1} \mathbf{h}_{[q,t]}^{\text{UR}} \in \mathbb{C}^{M_{\text{sub}} \times 1}. \quad (14)$$

In the subsequent time blocks, we estimate the piecewise small-timescale effective channels  $\{\mathbf{d}_{[q,t]} : q \in [Q], t \in [T-1]\}$ . This estimation is significantly simpler than directly estimating the piecewise effective channels  $\{\mathbf{H}_{[q,t]}^{\text{PW}} : q \in [Q], t \in [T-1]\}$  with the SOTA method or the coefficient matrices with 2TCE-PWCLRA. Toward this, we first describe the beam training method to derive suitable observations for our channel estimation method.

##### A. Piecewise Beam Training

For each time block  $t$ , the proposed beam training proceeds with  $B \leq M_{\text{sub}}$  subframes, each containing  $Q$  pilot symbols.

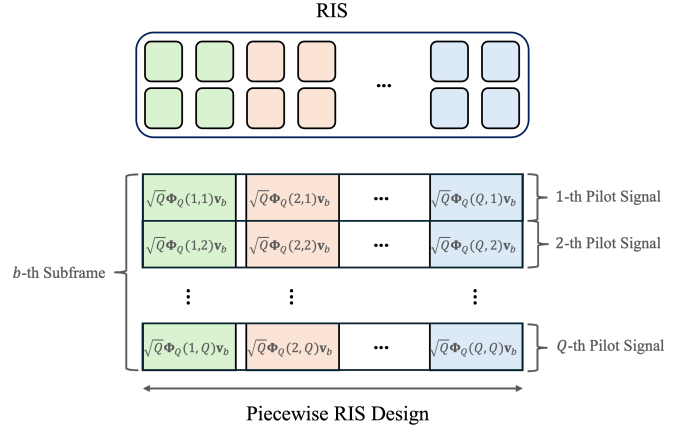


Fig. 2. The description of the proposed piecewise beam training, where  $\Phi_Q$  is a  $Q \times Q$  unitary matrix.

According to the signal model defined in (1), the BS receives the following signal during the  $i$ -th pilot transmission within the subframe  $b$ :

$$\mathbf{y}_{[b,i,t]} = \mathbf{W}^{\text{RF}} (\mathbf{H}^{\text{RB}} \text{diag}(\boldsymbol{\nu}_{[b,i,t]}) \mathbf{h}_t^{\text{UR}}) + \mathbf{n}_{[b,i,t]}, \quad (15)$$

where  $\boldsymbol{\nu}_{[b,i,t]}$  and  $\mathbf{n}_{[b,i,t]}$  denotes the RIS reflection vector and the additive noise, respectively. By dividing by the known pilot symbol, we can obtain:

$$\begin{aligned} \tilde{\mathbf{y}}_{[b,i,t]} &= \mathbf{W}^{\text{RF}} \mathbf{H}_t^{\text{eff}} \boldsymbol{\nu}_{[b,i,t]} + \tilde{\mathbf{n}}_{[b,i,t]} \\ &\stackrel{(a)}{=} \mathbf{W}^{\text{RF}} \sum_{q=1}^Q \mathbf{H}_{[q,t]}^{\text{PW}} \boldsymbol{\nu}_{[b,i,t]}(\mathcal{M}_q) + \tilde{\mathbf{n}}_{[b,i,t]}, \end{aligned} \quad (16)$$

where  $\tilde{\mathbf{n}}_{[b,i,t]} = \frac{1}{s} \mathbf{W}^{\text{RF}} \mathbf{n}_{[b,i,t]}$  and (a) comes from the definition of the piecewise effective channels in (6).

To derive piecewise observations via beam training, we construct the RIS reflection vector in a piecewise manner as illustrated in Fig. 2, adhering to the constant modulus constraint in (3):

$$\boldsymbol{\nu}_{[b,i,t]}(\mathcal{M}_q) = \sqrt{Q} \Phi_Q(q, i) \mathbf{v}_b \in \mathbb{C}^{M_{\text{sub}} \times 1} \quad (17)$$

for  $q \in [Q]$ , where  $\Phi_Q$  is a  $Q \times Q$  unitary matrix and  $\mathbf{v}_b$  is a  $M_{\text{sub}} \times 1$  vector. For each  $b \in [B]$ , we design the  $\mathbf{v}_b$  sequentially choosing the  $b$ -th column of an  $M_{\text{sub}} \times M_{\text{sub}}$  unitary matrix, such as discrete Fourier transform (DFT) matrix or Hadamard matrix. In Section IV-C, we will conduct a theoretical analysis to validate the effectiveness of our RIS design. Concatenating the  $Q$  received signals  $\{\tilde{\mathbf{y}}_{[b,i,t]} : i \in [Q]\}$ , we can define:

$$\begin{aligned} \mathbf{Z}_{[b,t]} &= \frac{1}{\sqrt{Q}} [\tilde{\mathbf{y}}_{[b,1,t]} \quad \cdots \quad \tilde{\mathbf{y}}_{[b,Q,t]}] \Phi_Q^{\text{H}} \\ &\stackrel{(a)}{=} \mathbf{W}^{\text{RF}} [\mathbf{H}_{[1,t]}^{\text{PW}} \mathbf{v}_b \quad \cdots \quad \mathbf{H}_{[Q,t]}^{\text{PW}} \mathbf{v}_b] + \tilde{\mathbf{U}}_{[b,t]}, \end{aligned} \quad (18)$$

where (a) is due to the fact that  $\Phi_Q$  is the unitary matrix and

$$\tilde{\mathbf{U}}_{[b,t]} = \frac{1}{\sqrt{Q}} [\tilde{\mathbf{n}}_{[b,1,t]} \quad \cdots \quad \tilde{\mathbf{n}}_{[b,Q,t]}] \Phi_Q^{\text{H}}. \quad (19)$$

Noticeably, as the number of pieces grows, the noise effect is reduced. In this paper, we refer to this effect as the beam

training gain. Ultimately, we obtain the piecewise observations as follows:

$$\begin{aligned} \mathbf{z}_{[b,q,t]} &\stackrel{\Delta}{=} \mathbf{Z}_{[b,t]}(:, q) \\ &= \mathbf{W}^{\text{RF}} \mathbf{H}_{[q,t]}^{\text{pw}} \mathbf{v}_b + \tilde{\mathbf{u}}_{[b,q,t]}, \end{aligned} \quad (20)$$

where  $\tilde{\mathbf{u}}_{[b,q,t]} = \tilde{\mathbf{U}}_{[b,t]}(:, q)$ . In the context of the proposed beam training, it is demanding to derive an optimal analog combiner  $\mathbf{W}^{\text{RB}}$  in terms of maximizing estimation accuracy. As a reasonable approach, we design the analog combiner using a fixed unitary matrix (e.g., DFT matrix or Hadamard matrix), which satisfies the constant modulus constraint in (3) and does not impact the noise distribution.

### B. Formulation of Multi-LS Problem

We formulate an optimization problem to efficiently estimate the small-timescale effective channels  $\{\mathbf{d}_{[q,t]} : q \in [Q], t \in [T-1]\}$  by utilizing the estimated effective channel in the initial time block, i.e.,  $\hat{\mathbf{H}}_0^{\text{eff}}$  in (10). Focusing on the  $q$ -th piecewise effective channel and the  $t$ -th time block, we delineate the proposed channel estimation problem. The same procedures will subsequently be applied to the other piecewise effective channels and time blocks. Based on the processed observations in (20) and the time-scaling property in (13), the small-timescale channels can be recovered through the formulation of a linear inverse problem:

$$\mathbf{z}_{[b,q,t]} = \mathbf{A}_{[b,q]} \mathbf{d}_{[q,t]} + \tilde{\mathbf{u}}_{[b,q,t]} \in \mathbb{C}^{N_{\text{RF}} \times 1}, \quad (21)$$

where the sensing (or measurement) matrix is formed by

$$\mathbf{A}_{[b,q]} \stackrel{\Delta}{=} \mathbf{W}^{\text{RF}} \hat{\mathbf{H}}_{[q,0]}^{\text{pw}} \text{diag}(\mathbf{v}_b) \in \mathbb{C}^{N_{\text{RF}} \times M_{\text{sub}}}. \quad (22)$$

We address this problem by pursuing an LS solution:

$$\mathbf{d}_{[q,t]}^{\text{LS}} = \arg \min_{\mathbf{d}} \|\mathbf{z}_{[b,q,t]} - \mathbf{A}_{[b,q]} \mathbf{d}\|_F^2. \quad (23)$$

According to the first-order optimality condition, an optimal solution must satisfy the normal equation:

$$\left( \mathbf{A}_{[b,q]}^H \mathbf{A}_{[b,q]} \right) \mathbf{d} = \mathbf{A}_{[b,q]}^H \mathbf{z}_{[b,q,t]}. \quad (24)$$

From the definition of  $\mathbf{A}_{[b,q]}$ , the Gram matrix can be specified as follows:

$$\begin{aligned} \mathbf{A}_{[b,q]}^H \mathbf{A}_{[b,q]} &= \text{diag}(\mathbf{v}_b^*) \left( \mathbf{W}^{\text{RF}} \hat{\mathbf{H}}_{[q,0]}^{\text{pw}} \right)^H \mathbf{W}^{\text{RF}} \hat{\mathbf{H}}_{[q,0]}^{\text{pw}} \text{diag}(\mathbf{v}_b) \\ &= (\text{diag}(\mathbf{v}_b^*) \mathbf{U}) \Lambda (\text{diag}(\mathbf{v}_b^*) \mathbf{U})^H \\ &\stackrel{(a)}{=} \sum_{i=1}^r \lambda_i (\mathbf{v}_b^* \circ \mathbf{u}_i) (\mathbf{v}_b^* \circ \mathbf{u}_i)^H \\ &\stackrel{(b)}{=} (\mathbf{v}_b \mathbf{v}_b^H) \circ \left( \left( \mathbf{W}^{\text{RF}} \hat{\mathbf{H}}_{[q,0]}^{\text{pw}} \right)^H \mathbf{W}^{\text{RF}} \hat{\mathbf{H}}_{[q,0]}^{\text{pw}} \right), \end{aligned} \quad (25)$$

where  $r \stackrel{\Delta}{=} \text{Rank}(\mathbf{W}^{\text{RF}} \hat{\mathbf{H}}_{[q,0]}^{\text{pw}}) = \min(N_{\text{RF}}, \hat{r}_q)$ ,

$$\left( \mathbf{W}^{\text{RF}} \hat{\mathbf{H}}_{[q,0]}^{\text{pw}} \right)^H \mathbf{W}^{\text{RF}} \hat{\mathbf{H}}_{[q,0]}^{\text{pw}} \stackrel{\Delta}{=} \mathbf{U} \Lambda \mathbf{U}^H = \sum_{i=1}^r \lambda_i \mathbf{u}_i \mathbf{u}_i^H \quad (26)$$

from the eigen-decomposition,  $\{\lambda_i : i \in [r]\}$  are positive eigenvalues, (a) comes from the fact

$$\text{diag}(\mathbf{v}_b^*) \mathbf{U} = [\mathbf{v}_b^* \circ \mathbf{u}_1 \quad \cdots \quad \mathbf{v}_b^* \circ \mathbf{u}_{M_{\text{sub}}}] \in \mathbb{C}^{M_{\text{sub}} \times M_{\text{sub}}},$$

and (b) is due to the distributive property of the Hadamard product. From (25) and the rank-inequality of the Hadamard product [32], the rank of the Gram matrix is bounded as follows:

$$\text{Rank} \left( \mathbf{A}_{[q,b]}^H \mathbf{A}_{[q,b]} \right) \leq \text{Rank} (\mathbf{v}_b \mathbf{v}_b^H) \min(N_{\text{RF}}, \hat{r}_q). \quad (27)$$

When  $B = 1$ , the Gram matrix is rank-deficient as  $\text{Rank} (\mathbf{v}_b \mathbf{v}_b^H) \min(N_{\text{RF}}, \hat{r}_q) = \min(N_{\text{RF}}, \hat{r}_q) < M$ . Consequently, we cannot derive a unique solution from the normal equation in (24). While an arbitrary solution can be obtained using QR-decomposition or singular value decomposition (SVD) [33], there is no assurance that this solution will approximate the desired one closely. Furthermore, the lack of a sparsity structure in the quasi-effective channel precludes the application of a compressed sensing (CS) framework.

From (27), it is evident that the rank of the Gram matrix can be increased by utilizing multiple observations (i.e.,  $B > 1$ ). Based on this intuition, we formulate a joint optimization problem, referred to as a multi-LS problem, utilizing the  $B > 1$  observations  $\{\mathbf{z}_{[b,q,t]} : b \in [B]\}$ :

$$\min_{\mathbf{d}} \sum_{b=1}^B \|\mathbf{z}_{[b,q,t]} - \mathbf{A}_{[b,q]} \mathbf{d}\|_F^2. \quad (28)$$

From the first-order optimality condition, we derive the normal equation for the multi-LS problem as follows:

$$\left( \sum_{b=1}^B \mathbf{A}_{[b,q]}^H \mathbf{A}_{[b,q]} \right) \mathbf{d} = \sum_{b=1}^B \mathbf{A}_{[b,q]}^H \mathbf{z}_{[b,q,t]}. \quad (29)$$

Extending the decomposition as described in (25) into the Gram matrix  $\mathbf{G}_q \stackrel{\Delta}{=} \sum_{b=1}^B \mathbf{A}_{[b,q]}^H \mathbf{A}_{[b,q]}$ , we obtain:

$$\begin{aligned} \mathbf{G}_q &= \sum_{b=1}^B \sum_{i=1}^r \lambda_i (\mathbf{v}_b^* \circ \mathbf{u}_i) (\mathbf{v}_b^* \circ \mathbf{u}_i)^H \\ &= \sum_{b=1}^B (\mathbf{v}_b \mathbf{v}_b^H) \circ \left( \left( \mathbf{W}^{\text{RF}} \hat{\mathbf{H}}_{[q,0]}^{\text{pw}} \right)^H \mathbf{W}^{\text{RF}} \hat{\mathbf{H}}_{[q,0]}^{\text{pw}} \right) \\ &\stackrel{(a)}{=} (\mathbf{V}_B \mathbf{V}_B^H) \circ \left( \left( \mathbf{W}^{\text{RF}} \hat{\mathbf{H}}_{[q,0]}^{\text{pw}} \right)^H \mathbf{W}^{\text{RF}} \hat{\mathbf{H}}_{[q,0]}^{\text{pw}} \right), \end{aligned} \quad (30)$$

where  $\mathbf{V}_B \in \mathbb{C}^{M_{\text{sub}} \times B}$  with  $B \leq M_{\text{sub}}$  is a full-rank matrix and (a) is due to the fact that  $\mathbf{V}_B \mathbf{V}_B^H = \sum_{b=1}^B \mathbf{v}_b \mathbf{v}_b^H$ . According to the rank-inequality in (27), the rank of the Gram matrix  $\mathbf{G}_q$  is bounded as follows:

$$\begin{aligned} \text{Rank} (\mathbf{G}_q) &\leq \text{Rank} (\mathbf{V}_B \mathbf{V}_B^H) \min(N_{\text{RF}}, \hat{r}_q) \\ &= B \min(N_{\text{RF}}, \hat{r}_q). \end{aligned} \quad (31)$$

To satisfy the necessary condition for obtaining a unique solution of the multi-LS problem in (28),  $B$  should be selected such that

$$B \geq \left\lceil \frac{M_{\text{sub}}}{\min(N_{\text{RF}}, \hat{r}_q)} \right\rceil = \left\lceil \frac{M}{Q \min(N_{\text{RF}}, \hat{r}_q)} \right\rceil. \quad (32)$$

Consequently, to hold the above necessary condition for all pieces, the minimum number of subframes, denoted as  $B_{\min}$ , should be determined as:

$$B_{\min} = \max_{q \in [Q]} \left\lceil \frac{M}{Q \min(N_{\text{RF}}, \hat{r}_q)} \right\rceil. \quad (33)$$

### C. Theoretical Analysis

We theoretically prove that under a mild condition,  $\mathbf{G}_q$  is full rank when  $B$  is selected as  $B \geq B_{\min}$ . Given the  $B$  reflection vectors  $\{\mathbf{v}_b : b \in [B]\}$ , we define the  $B$  subspaces of  $\mathbb{C}^{M_{\text{sub}}}$  as follows:

$$\mathcal{V}(\mathbf{v}_b^*) = \text{Span}(\text{diag}(\mathbf{v}_b^*)\mathbf{u}_1, \text{diag}(\mathbf{v}_b^*)\mathbf{u}_2, \dots, \text{diag}(\mathbf{v}_b^*)\mathbf{u}_r),$$

for  $b \in [B]$ . Note that for any fixed  $b \in [B]$ , the vectors  $\text{diag}(\mathbf{v}_b^*)\mathbf{u}_i$ ,  $i \in [r]$ , are linearly independent, i.e., these vectors form the basis of  $\mathcal{V}(\mathbf{v}_b^*)$ , because

$$\text{diag}(\mathbf{v}_b^*)(c_1\mathbf{u}_1 + c_2\mathbf{u}_2 + \dots + c_r\mathbf{u}_r) = \mathbf{0}, \quad (34)$$

only when the coefficients  $\{c_i : i \in [r]\}$  are all zeros due to the full-rankness of the diagonal matrix  $\text{diag}(\mathbf{v}_b^*)$ . To ensure that  $\text{Rank}(\mathbf{G}_q) = M_{\text{sub}}$ , the collection  $\{\mathcal{V}(\mathbf{v}_b^*) : b \in [B]\}$  should cover the vector space  $\mathbb{C}^{M_{\text{sub}}}$ , i.e.,

$$\bigcup_{b=1}^B \mathcal{V}(\mathbf{v}_b^*) = \mathbb{C}^{M_{\text{sub}}}. \quad (35)$$

Below, we provide a theoretical proof demonstrating that this condition is satisfied under a mild assumption, given that  $B \geq B_{\min}$ .

*Lemma 1:* For any pair of two distinct subframes  $b_1, b_2 \in [B]$  with  $b_1 \neq b_2$ , the  $2r$  number of vectors, represented as  $\{\text{diag}(\mathbf{v}_b^*)\mathbf{u}_i : b \in \{b_1, b_2\}, i \in [r]\}$ , are linearly independent if  $\mathcal{V}(\mathbf{v}_{b_1}^*) \neq \mathcal{V}(\mathbf{v}_{b_2}^*)$ .

*Proof:* By construction of  $\mathbf{v}_{b_1}$ ,  $\text{diag}(\mathbf{v}_{b_1}^*)\mathbf{U}$  is the unitary matrix. Therefore,  $\{\text{diag}(\mathbf{v}_{b_1}^*)\mathbf{u}_i : i \in [M_{\text{sub}}]\}$  are the orthonormal basis of  $\mathbb{C}^{M_{\text{sub}}}$ . Then, we obtain that for  $i \in [r]$ ,

$$\text{diag}(\mathbf{v}_{b_2}^*)\mathbf{u}_i = \sum_{j=1}^{M_{\text{sub}}} c_{[i,j]} \text{diag}(\mathbf{v}_{b_1}^*)\mathbf{u}_j \quad (36)$$

$$= \text{diag}(\mathbf{v}_{b_1}^*)\mathbf{U}\mathbf{c}_i, \quad (37)$$

where  $\mathbf{c}_i \in \mathbb{C}^{M_{\text{sub}} \times 1}$  denotes a coefficient vector. Concatenating the coefficient vectors,  $\mathbf{c}_1, \dots, \mathbf{c}_r$ , we define:

$$\begin{aligned} \mathbf{C} &= [\mathbf{c}_1 \quad \dots \quad \mathbf{c}_r] \\ &= (\text{diag}(\mathbf{v}_{b_1}^*)\mathbf{U})^H [\text{diag}(\mathbf{v}_{b_2}^*)\mathbf{u}_1 \quad \dots \quad \text{diag}(\mathbf{v}_{b_2}^*)\mathbf{u}_r]. \end{aligned} \quad (38)$$

Note that for  $i \in [r+1, M_{\text{sub}}]$ , the  $i$ -th row of  $\mathbf{C}$  is represented as follows:

$$\mathbf{C}(i, :) = (\text{diag}(\mathbf{v}_{b_1}^*)\mathbf{u}_i)^H [\text{diag}(\mathbf{v}_{b_2}^*)\mathbf{u}_1 \quad \dots \quad \text{diag}(\mathbf{v}_{b_2}^*)\mathbf{u}_r].$$

Thus,  $\mathbf{C}([r+1, M_{\text{sub}}], :)$  must not contain an all-zero row if

$$\mathcal{V}(\mathbf{v}_{b_1}^*) \neq \mathcal{V}(\mathbf{v}_{b_2}^*). \quad (39)$$

This is because  $\mathcal{V}(\mathbf{v}_{b_1}^*)$  is the orthogonal complement of the subspace, defined as  $\text{Span}(\text{diag}(\mathbf{v}_{b_1}^*)\mathbf{u}_{r+1}, \dots, \text{diag}(\mathbf{v}_{b_1}^*)\mathbf{u}_M)$ . This analysis implies that if  $\mathcal{V}(\mathbf{v}_{b_1}^*) \neq \mathcal{V}(\mathbf{v}_{b_2}^*)$ , any vector

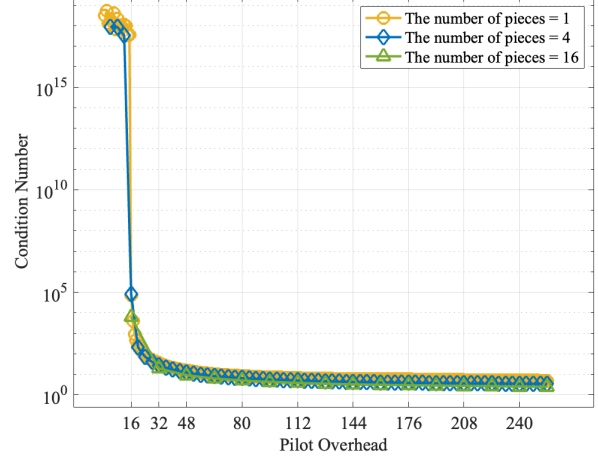


Fig. 3. The condition number of  $\mathbf{G}_q$  as a function of pilot overhead  $B$ .  $N = 64$ ,  $M = 256$ , and  $N_{\text{RF}} = 16$ .

of the set  $\{\text{diag}(\mathbf{v}_{b_2}^*)\mathbf{u}_i : i \in [r]\}$  must not be represented as a linear combination of the vectors in  $\{\text{diag}(\mathbf{v}_{b_1}^*)\mathbf{u}_i : i \in [r]\}$ . Also, from (34),  $\{\text{diag}(\mathbf{v}_{b_2}^*)\mathbf{u}_i : i \in [r]\}$  are linearly independent. This completes the proof. ■

Now we are ready to state our main theorem.

*Theorem 1:* Suppose that  $B \geq B_{\min}$ . Then, it is ensured that

$$\text{Rank}(\mathbf{G}_q) = M_{\text{sub}}, \quad (40)$$

if  $\mathcal{V}(\mathbf{v}_{b_1}^*) \neq \mathcal{V}(\mathbf{v}_{b_2}^*)$  for any  $b_1, b_2 \in [B]$  with  $b_1 \neq b_2$ .

*Proof:* From Lemma 1, we can see that the column space of  $\mathbf{G}_q$  is spanned by the linear combination of  $M_{\text{sub}}$  linearly independent vectors if  $\mathcal{V}(\mathbf{v}_{b_1}^*) \neq \mathcal{V}(\mathbf{v}_{b_2}^*)$  for any  $b_1, b_2 \in [B]$  with  $b_1 \neq b_2$ . This completes the proof. ■

To verify Theorem 1, we evaluate the condition number of the Gram matrix  $\mathbf{G}_q$  in (30), which is defined as:

$$\kappa(\mathbf{G}_q) \triangleq \log_{10} \left( \|\mathbf{G}_q\|_2 \|\mathbf{G}_q^{-1}\|_2 \right). \quad (41)$$

The condition number is identical to the ratio of the largest eigenvalue to the smallest eigenvalue of  $\mathbf{G}_q$ . When  $\kappa(\mathbf{G}_q)$  is large, thus,  $\mathbf{G}_q$  tends to be a singular matrix, which is referred to an ill-conditioned matrix. On the other hand,  $\mathbf{G}_q$  becomes a well-conditioned matrix as  $\kappa(\mathbf{G}_q) \rightarrow 0$ . Following the simulation settings in [26] (i.e., the simulation settings for 2TCE-FD), we conduct an experiment under the assumption that the RIS-BS channel  $\mathbf{H}^{\text{RB}}$  follows a general Rayleigh fading channel model, which can be represented by:

$$\text{vec}(\mathbf{H}^{\text{RB}}) \sim \mathcal{CN}(\mathbf{0}_{NM}, \rho^{\text{RB}} \mathbf{I}_{NM}). \quad (42)$$

Herein,  $\rho^{\text{RB}} = \rho_0 \left( \frac{d^{\text{RB}}}{d_0} \right)^{-\alpha^{\text{RB}}}$  represents the large-scale fading factor of the RIS-BS channel, where  $\rho_0$  denotes the large-scale path-loss at the reference distance  $d_0 = 1\text{m}$ , and we set  $\alpha^{\text{RB}} = 2.1$  and  $\alpha^{\text{UR}} = 4.2$ . Fig. 3 depicts the condition number  $\kappa(\mathbf{G}_q)$  as a function of pilot overhead  $QB$ . As expected, for  $QB < 16$ , meaning that the necessary condition in (32) is not satisfied regardless of the number of pieces  $Q \in \{1, 4, 16\}$ , the condition number becomes exceedingly

large, indicating that  $\mathbf{G}_q$  is a singular matrix. On the other hand, when the necessary condition holds (i.e.,  $QB \geq 16$ ), the condition number steeply decreases for all values of  $Q$ . Specifically, a phase transition occurs at  $B = B_{\min}$ . This reveals that the condition on  $\{\mathbf{v}_b : b \in [B]\}$  in Theorem 1 holds very well, namely,  $\mathbf{G}_q$  is full rank if  $B$  is chosen to be very close to  $B_{\min}$ .

#### D. The Proposed 2TCE-TSP

We describe the proposed channel estimation method. According to the necessary condition in (32), suppose that  $\text{Rank}(\mathbf{G}_q) = M_{\text{sub}}$  with a pilot overhead  $QB$  whose minimum is given by  $QB_{\min}$ . Then, we can derive the unique solution of the normal equation, such as

$$\mathbf{d}_{[q,t]}^{\text{LS}} = \mathbf{G}_q^{-1} \left( \sum_{b=1}^B \mathbf{A}_{[b,q]}^H \mathbf{z}_{[b,q,t]} \right). \quad (43)$$

In the intermediate and low SNR regimes, unfortunately, the noise amplification resulting from the multiplication of  $\mathbf{G}_q^{-1}$  should not be overlooked. In these regimes, the full rank of  $\mathbf{G}_q$  alone does not guarantee accurate estimation of the multiple-LS solution in (43). This is due to the inherent sensitivity of the estimation process to perturbations when the condition number  $\kappa(\mathbf{G}_q)$  is large. Consequently, a small amount of noise can lead to substantial inaccuracies in the estimates. This argument can be elucidated through the following mathematical derivation:

$$\begin{aligned} \Delta \mathbf{d}_{[q,t]}^{\text{LS}} &= \mathbf{G}_q^{-1} \left( \sum_{b=1}^B \mathbf{A}_{[b,q]}^H \mathbf{z}_{[b,q,t]} \right) \\ &\leq \|\mathbf{G}_q^{-1}\|_2 \left\| \sum_{b=1}^B \mathbf{A}_{[b,q]}^H \mathbf{z}_{[b,q,t]} \right\|_2 \\ &= \frac{10^{\kappa(\mathbf{G}_q)}}{\|\mathbf{G}_q\|_2} \left\| \sum_{b=1}^B \mathbf{A}_{[b,q]}^H \mathbf{z}_{[b,q,t]} \right\|_2, \end{aligned} \quad (44)$$

where  $\Delta \mathbf{d}_{[q,t]}^{\text{LS}}$  denotes the estimation error of the multiple-LS solution in (43). This demonstrates that the estimation error might increase exponentially with the condition number  $\kappa(\mathbf{G}_q)$ . Thus, one can enhance estimation accuracy by reducing the condition number through the appropriate selection of  $B \geq B_{\min}$ . In our simulations, we choose the  $B = 2B_{\min}$  or  $B = 3B_{\min}$  holding that  $QB \ll M$ .

## V. ANALYSIS

In this section, we describe the analysis of the computational complexity and the pilot overhead for the proposed small-timescale channel estimation method.

#### A. Computational Complexity

In the proposed small-timescale channel estimation method, the primary computational complexity arises from the matrix inversion required to derive the LS solution in (43). Accordingly, the computational complexity of the proposed method is obtained as  $\mathcal{O}(M^3/Q^2)$ . Table I provides a comparison of the computational complexities of the proposed and benchmark

TABLE I  
COMPARISONS OF MINIMUM PILOT OVERHEADS AND COMPUTATIONAL COMPLEXITIES PER EACH TIME BLOCK  $t \geq 1$

Algorithms	Minimum Pilot Overheads	Complexities
2TCE-TSP	$QB_{\min}$	$\mathcal{O}(M^3/Q^2)$
2TCE-FD	$M/\min(N_{\text{RF}}, \text{rank}(\mathbf{H}^{\text{RB}}))$	$\mathcal{O}(M^3)$
2TCE-PWCLRA	$M$	$\mathcal{O}\left(\sum_{q=1}^Q \hat{r}_q^3\right)$
2TCE-CLRA	$\lceil \text{rank}(\mathbf{H}^{\text{RB}}) / N_{\text{RF}} \rceil M$	$\mathcal{O}(\hat{r}^3)$

methods. Herein, the complexities of the 2TCE benchmark methods, based on CLRA algorithm, depend on the estimated rank of the RIS-BS channel, where  $\hat{r}_q$  and  $\hat{r}$  denote the estimated rank of  $\mathbf{H}_q^{\text{RB}}$  and  $\mathbf{H}^{\text{RB}}$ , respectively. In RIS-aided near-field communications, the RIS-BS channel exhibits a high-rank, which leads to an increase in both  $\hat{r}_q$  and  $\hat{r}$ . Nevertheless, these complexities are lower than that of the 2TCE-FD method and are comparable to the proposed 2TCE-TSP method when  $\mathbf{H}^{\text{RB}}$  becomes a full-rank matrix. Thus, it is asserted that the complexities of the CLRA-based method and the proposed method are nearly identical. Whereas, the complexity of the 2TCE-FD is regarded as having the highest computational complexity. To facilitate this comparison, Table II presents the run time for deriving the LS solution in the proposed method as a function of the number of RIS elements  $M$  and the number of pieces  $Q$ . It is observed that the run time increases as  $M$  grows and as  $Q$  decreases. Particularly when  $M$  is considerably large, the computational complexity tends to decrease rapidly as  $Q$  grows. In the worst case of  $Q = 1$ , it is noteworthy that the computational complexity of our method matches that of 2TCE-FD in [26]. By choosing  $Q > 1$ , we can significantly reduce the complexity of the proposed method. Moreover, this choice is justified as it alleviates the challenges posed by the high-rank of  $\mathbf{H}^{\text{RB}}$ . In conclusion, the proposed method, which employs piecewise estimation (i.e.,  $Q > 1$ ), effectively addresses the complexity issue arising from a large number of RIS elements, while preserving estimation accuracy.

TABLE II  
THE RUN TIME (SEC) FOR DERIVING THE LS SOLUTION ON THE NUMBER OF RIS ELEMENTS AND THE NUMBER OF PIECES.

	$M = 128$	$M = 256$	$M = 512$	$M = 1,024$
$Q = 1$	0.449	1.369	9.158	77.852
$Q = 2$	0.259	0.742	2.470	18.127
$Q = 4$	0.241	0.469	1.225	4.930
$Q = 8$	0.253	0.397	0.774	2.247
$Q = 16$	0.278	0.422	0.721	1.560

#### B. Pilot Overhead

Given  $N_{\text{RF}}$  and  $\text{Rank}(\mathbf{H}^{\text{RB}})$ , the pilot overhead, defined in (33), can be approximated as follows:



- When  $N_{\text{RF}} \leq \frac{\text{Rank}(\mathbf{H}^{\text{RB}})}{Q}$ , i.e., either  $\text{Rank}(\mathbf{H}^{\text{RB}})$  is very high or  $Q$  is relatively small, we can get:

$$QB_{\min} \approx \frac{M}{N_{\text{RF}}}. \quad (45)$$

Here, it is assumed that  $\hat{r}_q \approx \frac{\text{Rank}(\mathbf{H}^{\text{RB}})}{Q}$  for all  $q \in [Q]$ .

- When  $N_{\text{RF}} > \frac{\text{Rank}(\mathbf{H}^{\text{RB}})}{Q}$ , i.e.,  $\text{Rank}(\mathbf{H}^{\text{RB}})$  is relatively small, we can get:

$$QB_{\min} \approx \frac{M}{\text{Rank}(\mathbf{H}^{\text{RB}})/Q} \stackrel{(a)}{>} \frac{M}{N_{\text{RF}}}, \quad (46)$$

where (a) directly follows from  $N_{\text{RF}} > \frac{\text{Rank}(\mathbf{H}^{\text{RB}})}{Q}$ .

From (45) and (46), it is evident that  $Q$  must be selected as large as possible, ensuring that  $N_{\text{RF}} \leq \frac{\text{Rank}(\mathbf{H}^{\text{RB}})}{Q}$ . This choice can minimize the computational complexity, guaranteeing the minimum pilot overhead, such as  $\frac{M}{N_{\text{RF}}}$ . Given the system parameters  $N_{\text{RF}}$ , hence, we should carefully choose the number of pieces  $Q$  according to  $\text{rank}(\mathbf{H}^{\text{RB}})$ .

## VI. SIMULATION RESULTS

In our simulations, we focus on RIS-aided MU-MIMO systems, where  $N = 64$ ,  $M = 256$ , and  $N_{\text{RF}} = 16$ . Regarding the modeling of the RIS-BS channel, denoted as  $\mathbf{H}^{\text{RB}}$ , we will consider various channel models as outlined in [34]. The models we adopt are specified below:

- **UPW**: This is considered as a conventional far-field channel model, approximated with uniform channel gain and planar wavefronts (UPW). In mmWave or THz communications, this channel typically exhibits a sparse or low-rank structure, with the dominant path being the far-field line-of-sight (LoS) channel.
- **NUSW**: This is recognized as the most widely adopted model, approximated with non-uniform channel gain and spherical wavefronts (NUSW). Additionally, when a transmitter and a receiver are positioned within a certain distance known as Rayleigh distance (RD), this channel exhibits a near-field characteristic, demonstrating a higher rank compared to UPW.
- **SNS**: As the number of RIS extremely increases, a spatial non-stationary (SNS) channel arises due to the limited visual region (VR) of both the LoS and Non-LoS (NLoS) signal paths. This phenomenon results in a notably high rank for the RIS-BS channel, potentially achieving full rank. This represents a realistic channel model for RIS-aided near-field communications, particularly when the number of RIS elements is significantly high.

The UPW and NUSW channels are specifically modeled according to the physical settings in [34]. Additionally, the SNS channel is modeled by uniformly and randomly blocking 20% signals from the RIS to the BS. The User-RIS channel is also modeled according to one of the aforementioned channel models. The system frequency and the noise variance are set by 50 GHz and  $\sigma^2 = -169$  dBm, respectively.

As the metric to measure the channel estimation accuracy, we adopt the normalized mean square error (NMSE) according to the related works [17]–[22] as follows:

$$\text{NMSE} \triangleq \mathbb{E} \left[ \frac{1}{T} \sum_{t=1}^T \frac{\|\hat{\mathbf{H}}_t^{\text{eff}} - \mathbf{H}_t^{\text{eff}}\|^2}{\|\mathbf{H}_t^{\text{eff}}\|^2} \right], \quad (47)$$

where the estimated effective channels via the proposed method for a time block  $t \in [T - 1]$  are given by

$$\hat{\mathbf{H}}_t^{\text{eff}} = \left[ \hat{\mathbf{H}}_{[1,0]}^{\text{PW}} \text{diag}(\mathbf{d}_{[1,t]}^{\text{LS}}) \quad \cdots \quad \hat{\mathbf{H}}_{[Q,0]}^{\text{PW}} \text{diag}(\mathbf{d}_{[Q,t]}^{\text{LS}}) \right]. \quad (48)$$

We evaluate the expectation by Monte Carlo simulations with  $10^3$  trials, where the RIS-BS channel is fixed and the User-RIS channel is independently changed within all trials. That is, we can measure the mean performance of the proposed method for the rapidly varied small-timescale channel estimation. The signal-to-noise ratio (SNR) is defined as

$$\text{SNR} \triangleq 10 \log_{10} \left[ \frac{1}{T} \sum_{t=1}^T \frac{\|\mathbf{W}^{\text{RF}} \mathbf{H}^{\text{RB}} \text{diag}(\boldsymbol{\nu}_{[b,i]}) \mathbf{h}_t^{\text{UR},s}\|^2}{\|\mathbf{W}^{\text{RB}} \mathbf{n}_{[b,i,t]}\|^2} \right]. \quad (49)$$

Lastly, we assume that the initial large-timescale channel is perfectly estimated unless otherwise specified.

Fig. 4 illustrates the NMSE as a function of pilot overhead across various channel models. Notably, the results in Fig. 4(a) align closely with those in Fig. 3, indicating a significant decrease in the condition number as pilot overhead increases. This confirms the validity of our analysis regarding the relationship between estimation error and the condition number, as outlined in (44). Furthermore, the proposed 2TCE-TSP method demonstrates a substantial improvement over the existing 2TCE-FD proposed in [26] across all pilot overhead regimes. This substantiates the efficacy of our small-timescale channel estimation method, which leverages the time-scaling property alongside the PW-CLRA algorithm to significantly reduce pilot overhead while maintaining exceptionally low computational complexity, as analyzed in Table I and Table II. It is evident that as the number of pieces  $Q$  increases, the estimation accuracy improves due to the beam training gain of the piecewise beam training presented in (19). Additionally, for initial channel estimation, the proposed method is notably simpler and more practical than the 2TCE-FD method, which necessitates a full-duplex model. This further demonstrates the practicality of our channel estimation method.

In a high-frequency communications such as mmWave or THz, however, the Rayleigh fading channel model specified in (42) is impractical due to significant path loss. To consider more realistic channel models, Fig. 4(b), Fig. 4(c) and Fig. 4(d) plot the NMSE as the function of the pilot overhead for the UPW, NUSW and SNS channel models, respectively. We observe that the estimation accuracy improves with increasing pilot overhead across all channel models, as shown in Fig. 4(a). However, a performance loss appears to be unavoidable in real-world channel models compared to the performance of the Rayleigh fading channel model. From Fig. 4(b), we observe that the proposed method specifically struggles to estimate the channel in low pilot overhead regimes due to channel

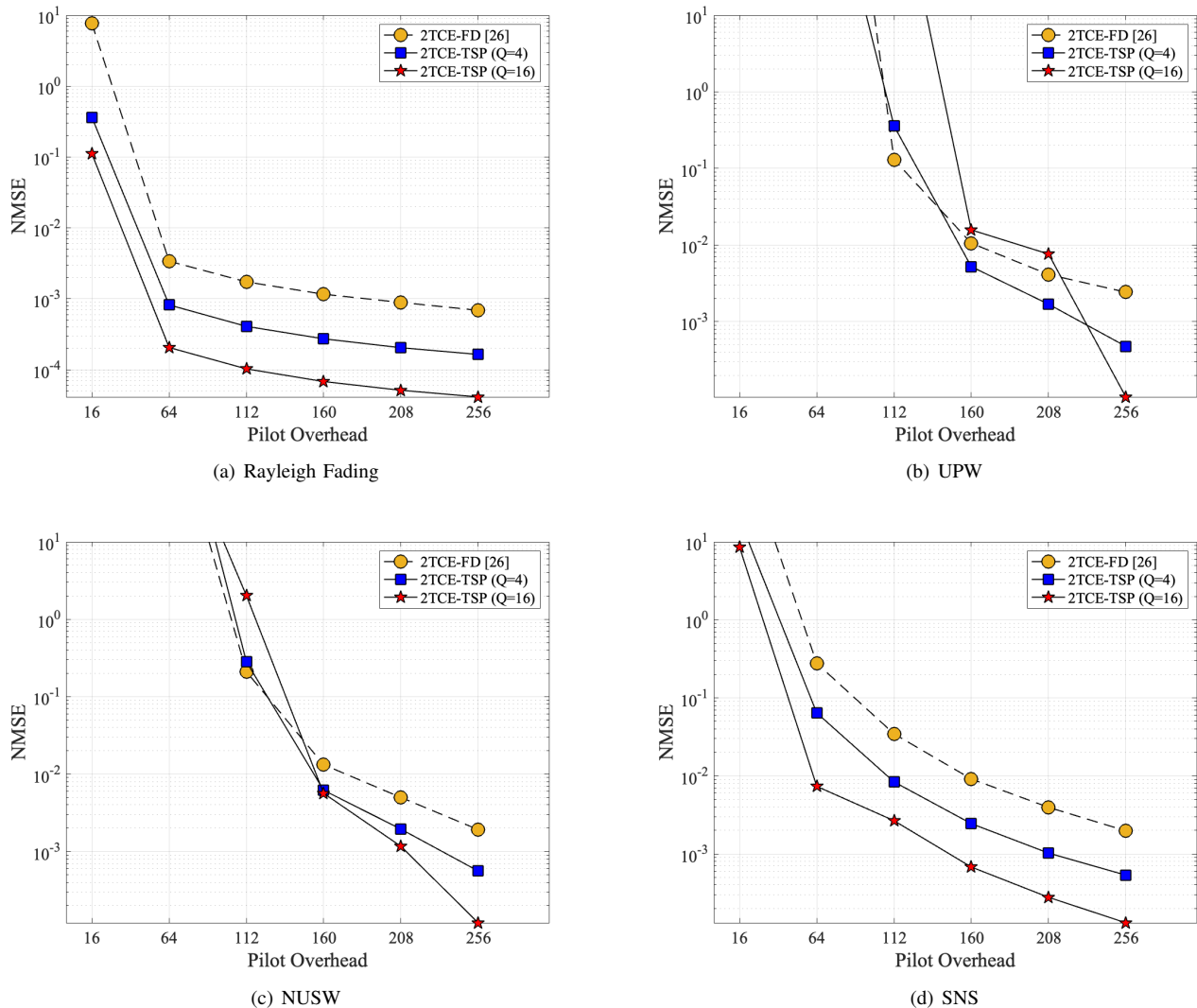


Fig. 4. The NMSE on the pilot overhead for various channel models. SNR = 20 dB.

sparsity. Also, the expected beam training gain associated with an increase in  $Q$  does not hold when pilot overhead is below 160. This is because the rank of each piece is significantly lower than the number of RF chains, specifically for the case of  $N_{\text{RF}} > \frac{\text{Rank}(\mathbf{H}^{\text{RB}})}{Q}$  in (46). Consequently, a greater pilot overhead is required. Therefore, it might be more appropriate to utilize CS-based methods [19], [20] for estimating small-timescale effective channels under certain assumptions.

In contrast to the UPW channel model, to the best of our knowledge, the proposed method shows the best performance for both NUSW and SNS channel models, which have a rank that exceeds that of the UPW channel model. From Fig. 4(c) and Fig. 4(d), we observe that estimation accuracy is significantly improved compared to the existing 2TCE-FD. When targeting accuracy of  $10^{-2}$ , the proposed method achieves the pilot overhead reduction of 50% for the NUSW channel model and 75% for the SNS channel model, relative to the maximum pilot overhead of  $M = 256$ , where the SOTA 2TCE-PWCLRA requires at least  $M = 256$  pilot overheads. Remarkably, the performance of our method for the SNS

channel model, which accounts for the limited visual region (VR) in relation to the NUSW channel model, surpasses that of the NUSW channel model. Therefore, the proposed method becomes more efficient for future near-field communications, as the impact of VR must be considered for channel modeling in near-field MIMO systems, especially as the number of RIS elements increases significantly.

Fig. 5 shows the NMSE as a function of SNR when  $Q = 16$ . Focusing on the SNS channel model, we observe that the proposed method outperforms the 2TCE-FD across all SNR regimes. Combining the results in Fig. 4, we can select the appropriate pilot overhead when a specific transmit power is provided. In the example where the target accuracy is  $10^{-3}$ , we require at least  $QB = 16 \times 8 = 128$  pilot overhead to achieve this accuracy at SNR = 20 dB. On the other hand, when SNR increases to 30dB, we can achieve the same accuracy using less pilot overhead, specifically  $QB = 16 \times 4 = 64$ . That is, we can achieve the target accuracy with much lower pilot overhead as SNR increases. Considering the trade-off between total power consumption and pilot overhead, we can identify

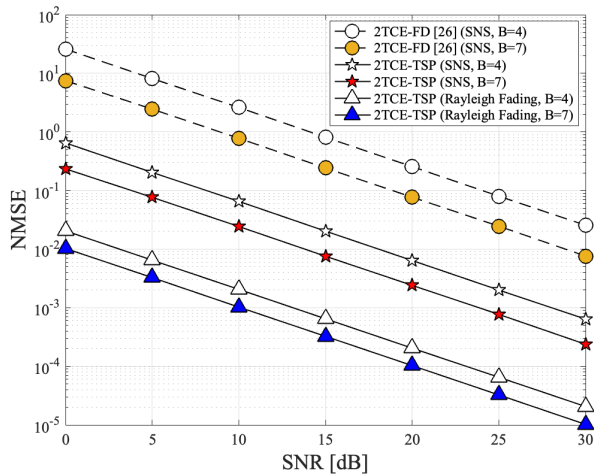


Fig. 5. The NMSE on SNR.  $Q = 16$ .

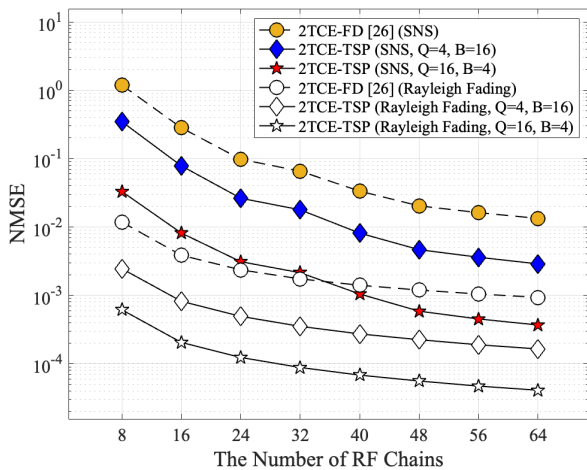


Fig. 6. The NMSE on the number of RF chains. SNR = 20 dB.

an optimal resource allocation.

Fig. 6 depicts the impact of the number of RF chains on the NMSE. We observe that for the same pilot overhead, the estimation accuracy increases as the number of RF chains grows. This is because from the equation in (30), the condition number of  $\mathbf{G}_q$  is enhanced as the column dimension of  $\mathbf{A}_{[b,q]}$  in (22) is expanded. This effect is similar to the MIMO zero-forcing receiver [35], where the increased number of antennas enhances the detection performance. Also, the proposed method outperforms the benchmark method presented in [26] across all the number of RF chains. Noticeably, the estimation accuracy for the SNS channel model is more sensitive to the number of RF chains than that of the Rayleigh fading channel model. This phenomenon is also observed in real-world channel models as shown in Fig. 4. Referred to the above results, therefore, we can design the system parameters like transmit power, the number of pieces and the number of RF chains considering the characteristic of each channel model.

Fig. 7 shows the NMSE on the pilot overhead in the

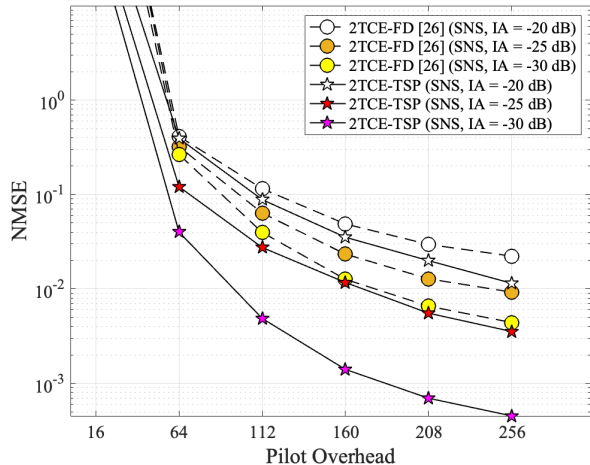


Fig. 7. The NMSE on pilot overhead in the presence of the initial channel estimation error.  $Q = 16$  and SNR = 20 dB.

presence of the initial channel estimation error, where we let “IA” in the legend denote the initial large-timescale channel estimation accuracy. Definitely, the estimation accuracy of the proposed method in the subsequent time blocks is notably improved as IA enhances. To efficiently utilize the proposed 2TCE-TSP method, hence, it is essential to accurately estimate the large-timescale channel during the initial time block. It is noteworthy that the benchmark 2TCE-FD algorithm necessitates full-duplex communications to estimate the large-timescale channel, resulting in significant pilot overhead and computational complexity. In contrast, the proposed method leverages time-scaling properties, enabling the 2TCE strategy with reduced overhead and complexity in practical scenarios such as time division duplexing (TDD) with half-duplexing.

Our experimental analysis suggests that the proposed 2TCE-TSP would be a good candidate for RIS-aided near-field communication systems owing to its attractive performance, lower overhead and complexity, and practicality.

## VII. CONCLUSION

We investigated the channel estimation problem for RIS-aided near-field communication systems. To effectively tackle the challenges of high pilot overhead and computational complexity associated with channel estimation, we implemented a two-timescale channel estimation strategy. This strategy leverages the time-scaling property and comprises both large-timescale and small-timescale channel estimations. Utilizing the existing PW-CLRA algorithm for large-timescale channel estimation, we formulate the multiple least-squares (multi-LS) problem. This problem aims to estimate the small-timescale effective channels by employing the previously estimated large-timescale channel alongside observations gathered through the proposed beam training method. Based on our theoretical analysis, we established the efficacy of the proposed beam training method and estimated the performance of our channel estimation method. Through simulations, we validated our theoretical analysis and demonstrated notable performances of the proposed method across various real-world channels.

## REFERENCES

- [1] S. Dang, O. Amin, B. Shihada, and M.-S. Alouini, "What should 6g be?" *Nature Electronics*, vol. 3, no. 1, pp. 20–29, 2020.
- [2] M. Chafii, L. Bariah, S. Muhaidat, and M. Debbah, "Twelve scientific challenges for 6g: Rethinking the foundations of communications theory," *IEEE Communications Surveys & Tutorials*, vol. 25, no. 2, pp. 868–904, 2023.
- [3] C.-X. Wang, X. You, X. Gao, X. Zhu, Z. Li, C. Zhang, H. Wang, Y. Huang, Y. Chen, H. Haas, J. S. Thompson, E. G. Larsson, M. D. Renzo, W. Tong, P. Zhu, X. Shen, H. V. Poor, and L. Hanzo, "On the road to 6g: Visions, requirements, key technologies, and testbeds," *IEEE Communications Surveys & Tutorials*, vol. 25, no. 2, pp. 905–974, 2023.
- [4] X. Wang, L. Kong, F. Kong, F. Qiu, M. Xia, S. Arnon, and G. Chen, "Millimeter wave communication: A comprehensive survey," *IEEE Communications Surveys & Tutorials*, vol. 20, no. 3, pp. 1616–1653, 2018.
- [5] W. Jiang, Q. Zhou, J. He, M. A. Habibi, S. Melnyk, M. El-Absi, B. Han, M. D. Renzo, H. D. Schotten, F.-L. Luo, T. S. El-Bawab, M. Juntti, M. Debbah, and V. C. M. Leung, "Terahertz communications and sensing for 6g and beyond: A comprehensive review," *IEEE Communications Surveys & Tutorials*, vol. 26, no. 4, pp. 2326–2381, 2024.
- [6] E. D. Carvalho, A. Ali, A. Amiri, M. Angelichinoski, and R. W. Heath, "Non-stationarities in extra-large-scale massive mimo," *IEEE Wireless Communications*, vol. 27, no. 4, pp. 74–80, 2020.
- [7] M. Di Renzo, A. Zappone, M. Debbah, M.-S. Alouini, C. Yuen, J. De Rosny, and S. Tret'yakov, "Smart radio environments empowered by reconfigurable intelligent surfaces: How it works, state of research, and the road ahead," *IEEE journal on selected areas in communications*, vol. 38, no. 11, pp. 2450–2525, 2020.
- [8] X. Pei, H. Yin, L. Tan, L. Cao, Z. Li, K. Wang, K. Zhang, and E. Björnson, "Ris-aided wireless communications: Prototyping, adaptive beamforming, and indoor/outdoor field trials," *IEEE Transactions on Communications*, vol. 69, no. 12, pp. 8627–8640, 2021.
- [9] Q. Wu, S. Zhang, B. Zheng, C. You, and R. Zhang, "Intelligent reflecting surface-aided wireless communications: A tutorial," *IEEE transactions on communications*, vol. 69, no. 5, pp. 3313–3351, 2021.
- [10] X. Mu, J. Xu, Y. Liu, and L. Hanzo, "Reconfigurable intelligent surface-aided near-field communications for 6g: Opportunities and challenges," *IEEE Vehicular Technology Magazine*, vol. 19, no. 1, pp. 65–74, 2024.
- [11] S. Lv, Y. Liu, X. Xu, A. Nallanathan, and A. L. Swindlehurst, "Ris-aided near-field mimo communications: Codebook and beam training design," *IEEE Transactions on Wireless Communications*, vol. 23, no. 9, pp. 12 531–12 546, 2024.
- [12] H. Zhou, M. Erol-Kantarci, Y. Liu, and H. V. Poor, "A survey on model-based, heuristic, and machine learning optimization approaches in ris-aided wireless networks," *IEEE Communications Surveys & Tutorials*, vol. 26, no. 2, pp. 781–823, 2024.
- [13] Z. Zhou, X. Gao, J. Fang, and Z. Chen, "Spherical wave channel and analysis for large linear array in los conditions," in *2015 IEEE Globecom Workshops (GC Wkshps)*, 2015, pp. 1–6.
- [14] M. Cui and L. Dai, "Channel estimation for extremely large-scale mimo: Far-field or near-field?" *IEEE Transactions on Communications*, vol. 70, no. 4, pp. 2663–2677, 2022.
- [15] —, "Near-field wideband beamforming for extremely large antenna arrays," *IEEE Transactions on Wireless Communications*, vol. 23, no. 10, pp. 13 110–13 124, 2024.
- [16] M. Cui, L. Dai, Z. Wang, S. Zhou, and N. Ge, "Near-field rainbow: Wideband beam training for xl-mimo," *IEEE Transactions on Wireless Communications*, vol. 22, no. 6, pp. 3899–3912, 2023.
- [17] J. Chen, Y.-C. Liang, H. V. Cheng, and W. Yu, "Channel estimation for reconfigurable intelligent surface aided multi-user mmwave mimo systems," *IEEE Transactions on Wireless Communications*, no. 10, pp. 6853–6869, 2023.
- [18] R. Schroeder, J. He, and M. Juntti, "Channel estimation for hybrid ris aided mimo communications via atomic norm minimization," in *2022 IEEE International Conference on Communications Workshops (ICC Workshops)*. IEEE, 2022, pp. 1219–1224.
- [19] S. Yang, W. Lyu, Z. Hu, Z. Zhang, and C. Yuen, "Channel estimation for near-field xl-ris-aided mmwave hybrid beamforming architectures," *IEEE Transactions on Vehicular Technology*, vol. 72, no. 8, pp. 11 029–11 034, 2023.
- [20] S. Yang, C. Xie, W. Lyu, B. Ning, Z. Zhang, and C. Yuen, "Near-field channel estimation for extremely large-scale reconfigurable intelligent surface (xl-ris)-aided wideband mmwave systems," *IEEE Journal on Selected Areas in Communications*, vol. 42, no. 6, pp. 1567–1582, 2024.
- [21] J. Lee, H. Chung, Y. Cho, S. Kim, and S. Hong, "Near-field channel estimation for xl-ris assisted multi-user xl-mimo systems: Hybrid beamforming architectures," *IEEE Transactions on Communications*, pp. 1–1, 2024.
- [22] J. Lee and S. Hong, "Near-field los/nlos channel estimation for ris-aided mu-mimo systems: Piece-wise low-rank approximation approach," 2024. [Online]. Available: <https://arxiv.org/abs/2410.13806>
- [23] C.-R. Tsai, Y.-H. Liu, and A.-Y. Wu, "Efficient compressive channel estimation for millimeter-wave large-scale antenna systems," *IEEE Transactions on Signal Processing*, vol. 66, no. 9, pp. 2414–2428, 2018.
- [24] Y. Lu and L. Dai, "Near-field channel estimation in mixed los/nlos environments for extremely large-scale mimo systems," *IEEE Transactions on Communications*, vol. 71, no. 6, pp. 3694–3707, 2023.
- [25] X. Zhang and J. Zheng, "Non-stationary near-field channel estimation for xl-mimo systems with hybrid combining," *IEEE Wireless Communications Letters*, vol. 13, no. 10, pp. 2727–2731, 2024.
- [26] C. Hu, L. Dai, S. Han, and X. Wang, "Two-timescale channel estimation for reconfigurable intelligent surface aided wireless communications," *IEEE Transactions on Communications*, vol. 69, no. 11, pp. 7736–7747, 2021.
- [27] S. Palmucci, A. Guerra, A. Abrardo, and D. Dardari, "Two-timescale joint precoding design and ris optimization for user tracking in near-field mimo systems," *IEEE Transactions on Signal Processing*, vol. 71, pp. 3067–3082, 2023.
- [28] K. Zhi, C. Pan, H. Ren, K. Wang, M. El-kashlan, M. D. Renzo, R. Schober, H. V. Poor, J. Wang, and L. Hanzo, "Two-timescale design for reconfigurable intelligent surface-aided massive mimo systems with imperfect csi," *IEEE Transactions on Information Theory*, vol. 69, no. 5, pp. 3001–3033, 2023.
- [29] E. Ahmed and A. M. Eltawil, "All-digital self-interference cancellation technique for full-duplex systems," *IEEE Transactions on Wireless Communications*, vol. 14, no. 7, pp. 3519–3532, 2015.
- [30] F. Zhu, F. Gao, T. Zhang, K. Sun, and M. Yao, "Physical-layer security for full duplex communications with self-interference mitigation," *IEEE Transactions on Wireless Communications*, vol. 15, no. 1, pp. 329–340, 2015.
- [31] A. Masmoudi and T. Le-Ngoc, "Channel estimation and self-interference cancelation in full-duplex communication systems," *IEEE Transactions on Vehicular Technology*, vol. 66, no. 1, pp. 321–334, 2016.
- [32] T. Ando, R. A. Horn, and C. R. Johnson, "The singular values of a hadamard product: A basic inequality," *Linear and Multilinear Algebra*, vol. 21, no. 4, pp. 345–365, 1987.
- [33] G. Strang, "Linear algebra and its applications," 2000.
- [34] H. Lu, Y. Zeng, C. You, Y. Han, J. Zhang, Z. Wang, Z. Dong, S. Jin, C.-X. Wang, T. Jiang, X. You, and R. Zhang, "A tutorial on near-field xl-mimo communications toward 6g," *IEEE Communications Surveys & Tutorials*, vol. 26, no. 4, pp. 2213–2257, 2024.
- [35] D. Tse and P. Viswanath, *Fundamentals of wireless communication*. Cambridge university press, 2005.